STUDY OF JET QUENCHING IN HEAVY ION COLLISIONS WITH THE ATLAS DETECTOR* **

Helena Santos

for the ATLAS Collaboration

LIP — Laboratório de Instrumentação e Física Experimental de Partículas
Av. Elias Garcia 14-1°, 1000-149 Lisboa, Portugal

(Received July 12, 2013)

Jets production in ultra-relativistic heavy ion collisions provides understanding of the mechanisms responsible for the hard scattered partons energy loss while crossing the hot and dense medium. The large acceptance and high granularity of the ATLAS Detector is well suited to study the phenomenon of jet suppression, namely its dependence on the jet transverse momentum and size, as well as the internal structure modification. Measurements of these observables provided by the Pb+Pb collision data collected during the 2010 and 2011 LHC runs, at the nucleon–nucleon center-of-mass energy of 2.76 TeV, are presented.

DOI:10.5506/APhysPolBSupp.6.923
PACS numbers: 12.38.Aw, 25.75.Nq

1. Introduction

Predictions from lattice QCD and evidences from ultra-relativistic Pb+Pb collisions data suggest that under extreme temperature and density, matter undergoes to a phase transition from ordinary hadronic matter to a plasma of quarks and gluons, the QGP. Later this plasma, under its own pressure, expands and cools resulting in the recombination of the quarks into hadrons that reach the detectors carrying the information of the deconfined phase.

The Heavy Ion Program of the LHC uses lead beams colliding at the center-of-mass energy of 2.76 TeV per nucleon pair. Results shown in this conference used data collected in the fall of the years 2010 and 2011, with

* Presented at the Workshop "Excited QCD 2013", Bjelašnica Mountain, Sarajevo, Bosnia–Herzegovina, February 3–9, 2013.

** This work was supported in part by FCT, UE, COMPETE and QREN under the contract Project CERN/FP/1116346/2010.

a total integrated luminosity of 7 μb^{-1} and 160 μb^{-1} respectively, which corresponds to 95% of the luminosity provided by the LHC. The performance of the ATLAS [1] was excellent during the data taking: the full detector was operational and the fraction of data passing quality criteria in each sub-detector was almost 100%. The collisions centrality, characterized by the overlap volume of the two colliding nuclei, has been estimated using the total transverse energy deposited in the forward calorimeters, $\sum E_{\mathrm{T}}^{\mathrm{Fcal}}$ (FCal, $3.2 \leq |\eta| < 4.9$). An analysis of the $\sum E_{\mathrm{T}}^{\mathrm{Fcal}}$ distribution after application of all trigger and selection requirements gives an estimate of the fraction of the sampled non-Coulomb inelastic cross section of $f = 98 \pm 2\%$. This estimate was derived from comparisons between measured and simulated $\sum E_{\mathrm{T}}^{\mathrm{Fcal}}$ distributions. The latter was obtained from a convolution of $\sqrt{s} = 2.76$ TeV $p + p$ data with a Monte Carlo Glauber model of the number of binary nucleon–nucleon collisions [2]. Using this fraction, data are divided into intervals corresponding to successive 10% percentiles.

Jet production is one of the hot topics of the heavy ion program. The interaction of the partons with the medium is expected to reduce the jet yields [3], as well as to modify the fragmentation functions [4]. The first indication of jet quenching at the LHC was given by the observation of large asymmetrical dijet events [5]. Later on, ATLAS extended these studies to γ–jet correlations [6]. However, these observables are not sensitive enough to provide a complete overview of the jet energy loss nature, so in order to improve the understanding on this fundamental issue, ATLAS performed measurements in the inclusive jet production as a function of the collisions centrality, jet transverse momentum and cone size [7], as well as in jet fragmentation functions [8]. Jets are reconstructed using the transverse energy of calorimeter "towers" as input signals for the anti-k_{t} algorithm [9], after subtracting the underlying event. The transverse energy associated to this contribution is estimated at event level in each calorimeter layer and strips of pseudorapidity, excluding regions containing jets. The flow modulation of the underlying event is taken into account in the estimates. Still, fluctuations in the background potentially produce reconstructed jets that do not originate from hard-scattering processes, mainly at low p_{T}. In order to reject these fake jets, additional matching requirement between "calorimeter" and "track" jets, as well as between "calorimeter" jets and electromagnetic energy clusters, is applied [7].

2. γ–jet correlations

An interesting observable to probe jet energy loss is to measure the jet energy relatively to the prompt photon energy, as the photon does not suffer from strong interaction and will emerge untouched from the fireball [10].

The top four plots of figure 1 show the ratio between the jet p_{T} and the photon p_{T}, $x_{J\gamma}$. The kinematic cuts applied to photons are $60 < p_{\mathrm{T}}^{\gamma} < 90$ GeV and $|\eta_{\gamma}| < 1.3$, while to jets are $p_{\mathrm{T}}^{\mathrm{jet}} > 25$ GeV and $|\eta_{\mathrm{jet}}| < 2.1$. The opening azimuthal angle between the photon and the jet, $\Delta\phi_{J\gamma}$, must be larger than $7\pi/8$. Anti-k_{t} jet parameter size is $R = 0.2$. Although not shown here, the results for larger jets, as $R = 0.3$, are quite similar. No jet efficiency corrections are applied, but each event is weighted by the inverse of the total photon efficiency. In order to correct the measured distribution of $x_{J\gamma}$ for the jet energy resolution, the distributions are unfolded following the singular-value decomposition of the response matrix (SVD) approach [11]. In peripheral collisions, data and simulation agree well, but an increasing discrepancy develops with the collisions centrality, a behavior already observed in dijet correlation measurement [5]. Monte Carlo simulation has no quenching effects into account. The azimuthal correlation between the γ and the jet, $\Delta\phi_{J\gamma}$, is shown in the bottom panels of figure 1. Despite the large imbalance between the jet p_{T} and the photon p_{T}, they remain back-to-back. Details on this analysis can be found in [6].

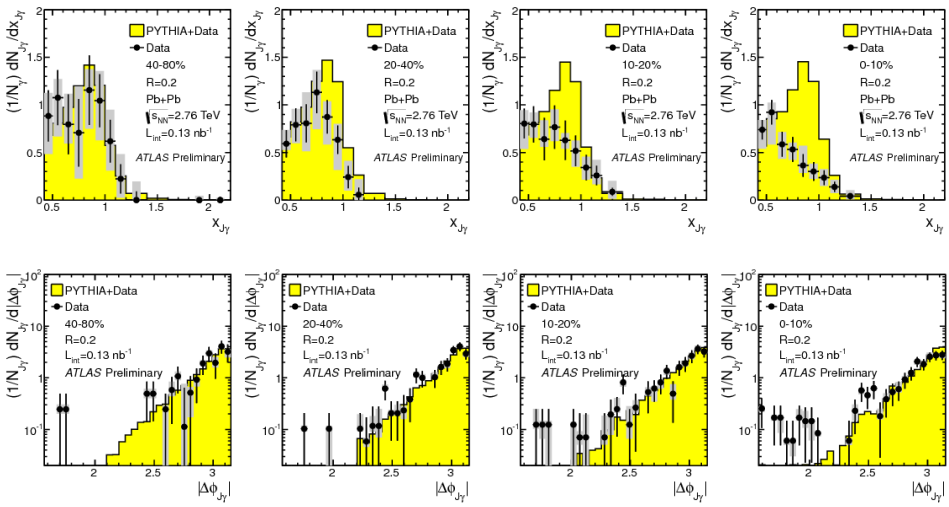


Fig. 1. Corrected $x_{J\gamma}$ distributions (top) and $\Delta\phi_{J\gamma}$ distributions (bottom) from Pb+Pb data (closed symbols) compared with PYTHIA (histogram) simulated events. Different collisions centrality intervals are shown, from left to right: 40–80%, 20–40%, 10–20% and 0–10%. The error bars represent statistical errors, while the gray bands indicate the systematic uncertainties [6].

3. Inclusive jet $R_{\rm cp}$

Although the dijet asymmetry and imbalanced γ–jet transverse momentum strongly suggest parton energy loss, other observables with more sensitivity to quenching effects are needed. Among them, the modifications of the inclusive jet $p_{\rm T}$ spectra contributes significantly to the understanding of the dependence of the suppression on jet energy, jet cone size and collisions centrality. These modifications are quantified using the so-called $R_{\rm cp}$ which is the ratio of the per-event jet yields divided by the number of binary nucleon–nucleon collisions, $N_{\rm coll}$, in a given centrality interval to the same quantity in a peripheral centrality one

$$R_{\rm cp}(p_{\rm T})|_{\rm cent} = \frac{\frac{1}{N_{\rm coll}^{\rm cent}}}{\frac{1}{N_{\rm coll}^{\rm per}}} \frac{\frac{N_{\rm jet}^{\rm cent}(p_{\rm T})}{N_{\rm evt}^{\rm cent}}}{\frac{N_{\rm jet}^{\rm per}(p_{\rm T})}{N_{\rm evt}^{\rm per}}} . \tag{1}$$

This ratio has also the advantage to cancel out systematic uncertainties independent of centrality. In the absence of quenching, the jet yields are expected to be proportional to $N_{\rm coll}$, and so the $R_{\rm cp}$ is expected to be 1. Jets

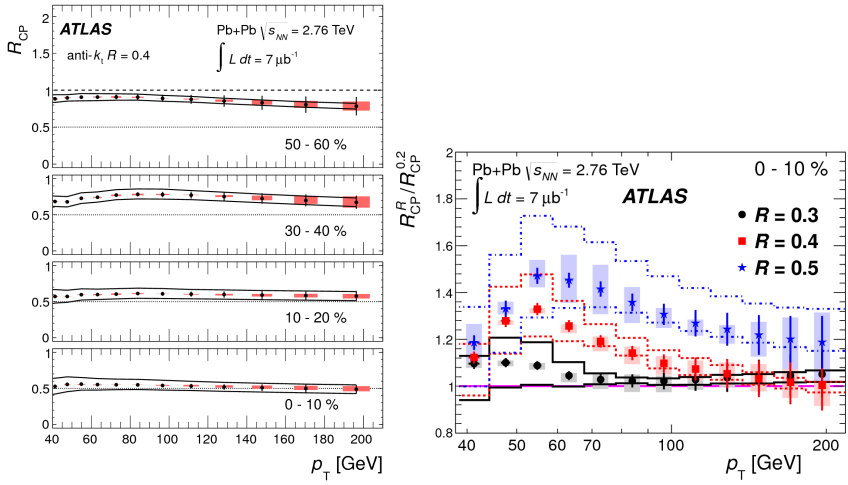


Fig. 2. Left: $R_{\rm cp}$ values as a function of jet $p_{\rm T}$ for $R = 0.4$ jets in four ranges of collisions centrality. The error bars represent statistical uncertainties from the unfolding, the shaded boxes indicate unfolding regularization systematic errors that are partially correlated between points. The solid lines indicate systematic errors that are fully correlated between all points. Right: Ratios of $R_{\rm cp}$ values between $R = 0.3$, 0.4 and 0.5 jets and $R = 0.2$ jets as a function of $p_{\rm T}$ in the 0–10% centrality interval. The error bars show statistical uncertainties. The shaded boxes indicate partially correlated systematic errors. The lines indicate systematic errors that are fully correlated between different $p_{\rm T}$ bins [7].

are reconstructed within $|\eta| < 2.1$ and required to have $38 \leq p_{\mathrm{T}} < 210$ GeV. The measured jet p_{T} spectra are corrected for bin migration effects using the unfolding technique of Ref. [11]. The left panel of figure 2 shows the inclusive jet R_{cp} for four centrality intervals, with the results in 60–80% used as the reference (see Eq. (1)). The suppression of the jet yields increases with collisions centrality reaching a factor of two in central collisions and shows little dependence on jet p_{T}. The right panel shows the ratios of R_{cp} values between $R = 0.3$, 0.4 and 0.5 jets and $R = 0.2$ jets as a function of jet p_{T} in the 0–10% centrality interval. The suppression is higher for narrower jets, which is consistent with a scenario where the lost energy is spread out over a larger angle [3]. Details on this analysis can be found in [7].

4. Jet fragmentation functions

Charged particle jet fragmentation functions provide insight in the modification of the longitudinal and transverse structure of the jet. For each charged particle, the longitudinal jet momentum fraction, z, is defined as $z = p_{\mathrm{T}}^{\mathrm{ch}}/p_{\mathrm{T}}^{\mathrm{jet}} \cos\Delta R$, where ΔR represents the angle between the charged particle and jet directions. The longitudinal fragmentation functions functions of z and p_{T} are defined as

$$D(z) = \frac{1}{N_{\mathrm{jet}}} \frac{dN_{\mathrm{ch}}(z)}{dz}, \qquad D(p_{\mathrm{T}}) = \frac{1}{N_{\mathrm{jet}}} \frac{dN_{\mathrm{ch}}(p_{\mathrm{T}})}{dp_{\mathrm{T}}}, \tag{2}$$

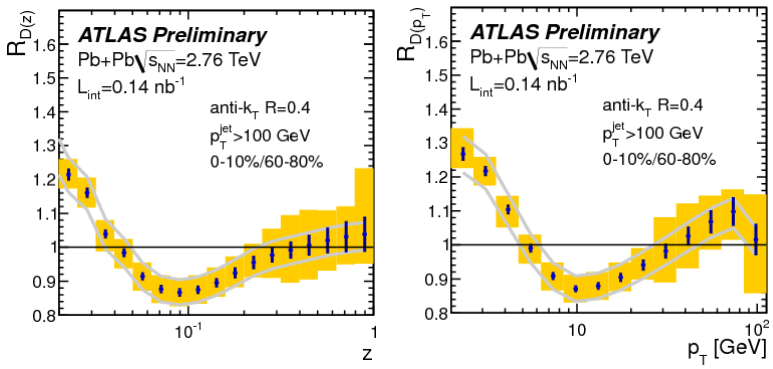


Fig. 3. Right: Ratio of unfolded $D(z)$ for central (0–10%) to peripheral (60–80%) collisions, $R_{D(z)}$, for $R = 0.4$ jets. The error bars represent statistical uncertainties while the shaded bands indicate systematic uncertainties that are uncorrelated or partially correlated between points. The solid lines indicate systematic uncertainties that are 100% correlated. Left: The same as in the right plot, but regarding ratios of unfolded $D(p_{\mathrm{T}})$ [8].

where $D(z)$ measures the p_{T} of charged particles parallel to the jet axis, whereas $D(p_{\mathrm{T}})$ is the p_{T} spectrum of the charged particles inside the jet. Jets reconstructed with the anti-k_{t} algorithm with radius set to 0.4 are required to have $|\eta| < 2.1$ and $p_{\mathrm{T}} > 100$ GeV. Measured charged particles have $p_{\mathrm{T}} > 2$ GeV and an angular range within $\Delta R < 0.4$ of the jet direction. The central (0–10%) to peripheral (60–80%) ratios of $D(z)$ and p_{T} are shown in the left and right panels of figure 3, respectively. An enhancement of particles at low z and low p_{T} is observed, whereas a suppression at $z \approx 0.1$ and $p_{\mathrm{T}} \approx 10$ GeV reaches 20%. No modification at high z and high p_{T} occurs, which contradicts some theoretical expectations [4]. Details on this analysis can be found in [8].

5. Conclusions

γ–jet correlation in peripheral collisions is compatible with non-quenching based Monte Carlo model, but an increasing disagreement between data and simulation with increasing collisions centrality is observed. The γ–jet correlation in azimuth remains back-to-back. Jet production is suppressed by a factor of two in central collisions with respect to peripheral; negligible dependence with jet p_{T} is observed. The suppression is larger for narrower jets, which is consistent with out-of-cone energy loss scenario. The jet structure is modified: there is an enhancement of particles at low z and p_{T}, whereas a suppression at intermediate z and p_{T} is observed. Although, these observations are well in agreement with the predictions, the absence of high suppression at high z contradicts some expectations.

REFERENCES

[1] ATLAS Collaboration, *JINST* **3**, S08003 (2008).
[2] M.L. Miller, K. Reygers, S.J. Sanders, P. Steinberg, *Annu. Rev. Nucl. Part. Sci.* **57**, 205 (2007).
[3] I. Vitev, S. Wicks, B.W. Zhang, *J. High Energy Phys.* **0811**, 093 (2008).
[4] N. Armesto, L. Cunqueiro, C.A. Salgado, W.C. Xiang, *J. High Energy Phys.* **0802**, 093 (2008).
[5] ATLAS Collaboration, *Phys. Rev. Lett.* **105**, 252303 (2010).
[6] ATLAS Collaboration, ATLAS-CONF-2012-121, `https://cdsweb.cern.ch/record/1473135`
[7] ATLAS Collaboration, *Phys. Lett.* **B719**, 220 (2013).
[8] ATLAS Collaboration, ATLAS-CONF-2012-115, `https://cdsweb.cern.ch/record/1472936`
[9] M. Cacciari, G.P. Salam, G. Soyez, *J. High Energy Phys.* **0804**, 063 (2008).
[10] X.-N. Wang, Z. Huang, I. Sarcevic, *Phys. Rev. Lett.* **77**, 231 (1996).
[11] A. Hocker, V. Kartvelishvili, *Nucl. Instrum. Methods* **A372**, 469 (1996).